Post-contrast 3D T1-weighted TSE MR sequences (SPACE, CUBE, VISTA/BRAINVIEW, isoFSE, 3D MVOX): Technical aspects and clinical applications

Blanche Bapst, Jean-Louis Amegnizin, Alexandre Vignaud, Paul Kauv, Anne Maraval, Erwah Kalsoum, Titien Tuilier, Azzedine Benaissa, Pierre Brugières, Xavier Leclerc, et al.

Version of Record: https://www.sciencedirect.com/science/article/pii/S0150986120301115
Manuscript_0de79bca9b08cece14e6c9320212c225

POST-CONTRAST 3D T1-WEIGHTED TSE MR SEQUENCES (SPACE, CUBE, VISTA/BRAINVIEW, isoFSE, 3D MVOX): TECHNICAL ASPECTS AND CLINICAL APPLICATIONS

Review Article

Blanche Bapst, MD [1], Jean-Louis Amegnizin, MD [1], Alexandre Vignaud, PhD [2], Paul Kauv, MD, PhD [1], Anne Maraval, MD [1], Erwah Kalsoum, MD [1], Titien Tuilier, MD [1], Azzedine Benaissa, MD [1], Pierre Brugières, MD [1], Xavier Leclerc, MD, PhD [3], Jérôme Hodel, MD, PhD [1]

(1) Service de Neuroradiologie, CHU Henri Mondor, Créteil

(2) CEA, Neurospin, Saclay

(3) Service de Neuroradiologie, CHRU Lille

Corresponding author:

Jérôme Hodel, Department of Neuroradiology

CHU Henri Mondor, Créteil, France

Tel: 033 149812641 Fax: 033 149812644

jerome.hodel@gmail.com

POST-CONTRAST 3D T1-W TSE MR SEQUENCES (SPACE, CUBE, VISTA/BRAINVIEW, isoFSE, 3D MVOX): TECHNICAL ASPECTS AND CLINICAL APPLICATIONS

Review article

Abstract

Post-contrast three-dimensional T1-weighted imaging of the brain is widely used for a broad range of vascular, inflammatory or tumoral diseases. The variable flip angle 3D TSE sequence is now available from several manufacturers (CUBE, General Electric; SPACE, Siemens; VISTA/BRAINVIEW, Philips; isoFSE, Itachi; 3D MVOX, Canon). Compared to gradient-echo (GRE) techniques, 3D TSE offers the advantages of useful image contrasts and reduction of artifacts from static field inhomogeneity. However, the respective role of 3D TSE and GRE MR sequences remains to be elucidated, particularly in the setting of post-contrast imaging. The purpose of this review was 1/ to describe the technical aspects of 3D TSE sequences, 2/ to illustrate the main clinical applications of the post-contrast T1-w 3D TSE sequence through clinical cases, 3/ to discuss the respective role of post-contrast 3D TSE and GRE imaging in the field of neuroimaging.

ABBREVIATIONS

- 3D T1-w: three-dimensional T1-weighted
- TSE: turbo spin echo
- GRE: gradient echo
- MSDE: motion-sensitized driven equilibrium
- DANTE: delay alternating with nutation for tailored excitation
- VW-MRI: vessel-wall MR imaging

INTRODUCTION

Post-contrast three-dimensional T1-weighted (3D T1-w) imaging of the brain is increasingly used in clinical routine for a broad range of neurovascular, inflammatory or tumoral diseases. In the daily practice, both spin-echo (SE) and gradient-echo (GRE)-based MR sequences are available to achieve post-contrast imaging.

The variable flip angle 3D turbo spin-echo (TSE) MR sequence is now routinely available from several manufacturers (CUBE, General Electric; SPACE, Siemens; VISTA/BRAINVIEW, Philips; isoFSE, Hitachi; and 3D MVOX, Canon). Such a SE-based acquisition offers the advantages of useful image contrasts (including T1-w, T2-w, PD-w, FLAIR or DIR) and reduction of artifacts from static field inhomogeneity (1-3). However, the respective role of 3D TSE and GRE MR sequences is poorly reported in the literature.

From 2010 to 2019, we routinely performed both TSE and GRE post-contrast 3D T1-w imaging of the brain, for a broad range of vascular, inflammatory or tumoral diseases, using

different 3T MR scanners and TSE sequences (CUBE, Discovery MR750, GE Healthcare, Milwaukee; SPACE, Verio and Skyra, Siemens, Erlangen, Germany; VISTA/BRAINVIEW, Achieva and Ingenia, Philips Healthcare, Best, the Netherlands). The 3D T1-w GRE imaging used included (i) non-EPI fast GRE sequence (FFE, Philips Healthcare, Best, the Netherlands; SPGR, GE Healthcare, Milwaukee, Wisconsin; FLASH, Siemens, Erlangen, Germany) or (ii) with a ultrafast GRE sequence including a magnetization-preparation (TFE, Philips Healthcare, Best, the Netherlands; BRAVO, General Electric, Milwaukee, Wisconsin; MP-RAGE, Siemens, Erlangen, Germany). A standard dose of gadolinium (0.1 mmol/kg), either gadoterate meglumine (Dotarem; Guerbet, France) or gadobutrol (Gadovist; Bayer Pharmaceuticals, Berlin, Germany), was used. The post-contrast T1-w imaging was acquired at least 5-minute after gadolinium administration in all cases.

The reported illustrative cases were selected and analyzed by a panel of senior neuroradiologists. The purpose of this review article is 1/ to describe the technical aspects of 3D TSE sequences, 2/ to illustrate the main clinical applications of the post-contrast 3D T1-w TSE sequence through clinical cases, 3/ to discuss the respective role of post-contrast 3D T1-w and GRE imaging in the field of neuroimaging.

TECHNICAL ASPECTS

It is well known that post-contrast 2D T1-w GRE images usually provide lower contrast than SE on a large spectrum of brain lesions (4). However, post-contrast GRE 3D T1-w imaging regained interest in the community due to the wider availability of 3T MRI and the introduction of isotropic 3D turbo-FLASH like approaches (also called “MPRAGE”) (5, 6).

Of note, the 3D T1-w TSE sequence was very challenging to implement (7), explaining why this sequence was introduced long after the 3D T2-w TSE and variants (8). Indeed, several limitations made it more challenging to perform the 3D TSE sequence T1-weighted. First, if a classic TSE scheme is selected to accelerate the k-space filling, long echo trains may result in sub-optimal image quality for T1-w contrast, since T2-weighting of the signals tends to develop along the echo train. In addition, T1-w contrast, low spatial-frequency signals are typically acquired earlier in the echo train than high spatial-frequency signals, and thus substantial image blurring will occur if the signal intensities for high spatial frequencies are significantly less than those for low spatial frequencies (7). Using T1-w images, blurring occurs when the echo length train is more that the T2 value of primary interest (9). Moreover, compared to T2-w sequences, the echo lengthening coupled with short TR made the sequence extremely demanding in terms of SAR (Specific Absorption Ratio).

Variable flip angles and echo-spacing. Modern 3D TSE sequences are characterized by (i) long echo-train with variable flip angle refocusing pulses that preserve T1-weighting integrity, (ii) ultra-short echo-spacing, and (iii) optimized k-space trajectories (with sampling in both in-plane and through-slab phase encode direction during signal evolution) (8). Variable refocusing flip angles are determined by calculating the target signal using the prospective extended phase graph algorithm (1). It also includes an optimized restore scheme to reduce as much as possible TR (7). Such approach improves the useable duration of the echo train and allows the use of very long spin-echo trains (1) with several advantages including (i) limited specific absorption rate (SAR), (ii) reduced artifacts from static field

inhomogeneity compared to 3D GRE based sequences and (iii) clinically acceptable scan times.

Power Deposition. The power deposition for a radio-frequency (RF) pulse varies as the square of the flip angle for the RF pulse (8). As previously reported, variable flip angle refocusing RF pulses offer the opportunity to significantly reduce SAR compared to conventional SE train (10).

Black blood effect and flow sensitivity. The 3D T1-w TSE sequence includes an intrinsic black-blood effect mainly related to intravoxel dephasing among the blood spins (11-13). As a result, brain vessel lumen appears mostly hypointense (the "black blood" effect) using this sequence (Figure 1). In the setting of post-contrast imaging, the black blood effect can be advantageous to suppress the vascular flow-related artifacts commonly encountered on 2D TSE (figure 2) (14). Of note, such black blood effect remains usually incomplete when using conventional 3D TSE sequences, being more pronounced within brain arteries and large dural sinuses, but potentially lacking in slow-flowing vessels such as cortical veins.

3D TSE images of the normal brain and comparison with GRE-based techniques. 3D TSE sequences differ from GRE-based imaging in terms of (i) image contrast, (ii) flow-sensitivity and (iii) artifacts from static field inhomogeneity. Indeed, 3D T1-w TSE is characterized by a very low contrast between the grey and white matter, while magnetization-prepared GRE techniques increase such contrast. Moreover, while proximal brain arteries usually appear hyperintense on GRE images, they are typically hypointense on TSE images due to the inherent black blood effect. Susceptibility artifacts are also less pronounced on TSE imaging. Differences between GRE and TSE images are illustrated in Figure 3.

Technical differences between post-contrast T1w 3D TSE and GRE MR sequences are summarized in Table 1.

OPTIMIZING THE POST-CONTRAST 3D T1-W TSE SEQUENCE

Fat saturation. Fat suppression, with a spectral pre-saturation with inversion recovery (SPIR) technique, is usually performed when using the 3D T1-w TSE sequence post-contrast. This is not the case when using GRE imaging. Recently, DIXON techniques (Cube IDEAL/Flex) have been introduced, potentially improving fat saturation homogeneity.

Increasing the black blood effect in 3D TSE images. As previously stated, residual blood signals can be encountered with the post-contrast 3D T1-w TSE sequence due to an incomplete suppression by intravoxel dephasing of slow-flowing blood (for example within cortical veins or in case of arterial stenosis) (15). Such residual vascular enhancement may

have clinical implications, being potentially mistaken with parenchymal enhancing lesions. However, the black blood effect can be further optimized/increased in TSE images by using additional preparation pulses. First by using "Motion-Sensitized Driven Equilibrium" (MSDE) preparation that uses flow-sensitive dephasing gradients with low b-values to suppress residual blood-flow (16). This approach uses a diffusion module with low b-values, so the sequence suppresses bulk flow rather than molecular diffusion. MSDE preparation was previously used for the imaging of brain aneurysms (17) or carotid wall (18, 19). Second, "Delay Alternating with Nutation for Tailored Excitation" (DANTE) preparation is another technique that uses a series of non-selective low flip angle pulses interleaved with gradient pulses, responsible of a spoiling effect where flowing spins cannot achieve steady-state (20-22). Using additional MSDE or DANTE preparation, the resulting TSE image consists in an almost complete lack of enhancement within slow-flowing veins (Figure 4). DANTE may represent a good compromise in terms of SAR reduction and time efficiency (21). While the black-blood techniques were initially designed for the imaging of vessel-wall, MSDE or DANTE preparation may also be useful to further improve the detection of brain enhancing lesion, encompassing a wide range of clinical applications. However, since these techniques are still not widely available, further clinical studies are required to assess the respective role of post-contrast 3D TSE acquired with and without additional black-blood techniques in the daily routine practice.

Further reducing the scan-time. The acquisition time depends mainly on the compromise between spatial resolution and SNR. It usually ranges between 4 to 5 minutes. Reducing scan-time is an important issue when using 3D TSE imaging. In fact the optimal echo train length (ETL) is constant for a given echo spacing and TR. Further increasing the ETL would require a compromise on image weighting and Point Spread Function (PSF), leading to blurring and

suboptimal contrast. Therefore, acquiring the minimum readout lines with a partial Fourier acquisition decreases the scan-time when using 3D TSE, but this approach also alters PSF. One strategy consists in 1D or 2D parallel acceleration, enhanced by high density phased array receiving coils (23). More recently introduced, the 2D CAIPIRINHIA technique (24), has significantly increased the acceleration factor of the 3D TSE sequence without significant artifacts (25).

Other strategies have been recently developed to further accelerate 3D TSE in 2D, including the "compressed sensing" (CS) technique. CS uses the sparsity of MR images to randomly undersample the *k*-space, thus saving scan time (26). Contrary to parallel imaging, CS is insensitive to the coil configuration. Because each acceleration technique imposes independent constraints on the image reconstruction, CS can be used in addition to parallel imaging (27). Such an approach appears very effective using 3D FLAIR for several clinical applications, including multiple sclerosis (MS) (28, 29) but may lead to additional blurring. Several iterative algorithms, similar to CS, are being developed with the advantage of being more adapted to the T1-weighted contrast. According to the acceleration factor used, the scan-time reduction may be about 33% with these techniques (28).

IMAGE INTERPRETATION

Thinner slices and multiplanar analysis. There are several advantages of using 3D thinner slices for the detection of brain-enhancing lesions. Thinner section images minimize the partial volume effect between small lesions and surrounding brain tissue (30-32). 3D

acquisitions, thanks to their higher signal to noise ratio (SNR) and isotropic voxel size, allow for maximal intensity projection (MIP) reformations in arbitrary planes (Figure 5). With the 3D TSE sequence, such MIP views can be routinely obtained due to the low contrast between gray and white matter, further improving the detection of enhancing lesions (33) (Figure 3).

Co-registration with other 3D sequences. Enhancement of brain vessels can be potentially misinterpret with parenchymal lesions, particularly when MSDE or DANTE preparation are not available. However, co-registration of the post-contrast 3D T1-w TSE sequence with 3D FLAIR and susceptibility-weighted imaging can improve the diagnostic work-up, avoiding such pitfall (Figure 6). Indeed, a brain lesion is usually associated with hyperintensity on T2w/FLAIR imaging while brain vessels can be easily recognized using SWI without associated T2w/FLAIR hyperintensity.

ADDED VALUE OF THE POST-CONTRAST 3D T1-W TSE SEQUENCE IN NEUROLOGICAL DISEASES

Parenchymal enhancing lesions: multiple sclerosis and brain tumors

Parenchymal gadolinium enhancement usually reflects brain blood barrier breakdown (with contrast leakage) and/or neo-angiogenesis. Several neurological diseases may lead to parenchymal enhancement, including multiple sclerosis and brain tumors.

Compared with GRE techniques at the same spatial resolution, the post-contrast 3D T1-w TSE sequence appears more sensitive for the detection of brain-enhancing lesions. This is explained by: (i) improved image contrast between gadolinium enhancing lesions and surrounding brain tissue; (ii)

higher signal-to-noise-ratio ; (iii) additional black blood effect and ;(iv) reduced artifacts from static field inhomogeneity (34-36).

Using the 3D TSE sequence, the signal-intensity of the grey and white matter is relatively similar and lower as compared to GRE images (which is associated with a high signal-intensity of the white matter). Thus, image contrast between contrast-enhanced lesions and surrounding brain tissue will be increased by the use of TSE imaging.

Several studies have previously suggested that 3D T1-w TSE is an alternative approach to MPRAGE (37), and even superior to GRE imaging for the detection of small brain enhancing lesions (17, 23, 38-40) or meningitis (41, 42), with comparable acquisition times. Interestingly, it was reported that thick-slab overlapping TSE reformatted MIP views can improve time-efficiency for the detection of small enhanced metastasis compared to GRE techniques (33). Recently, the added value of the post-contrast 3D T1-w TSE sequence with the DANTE preparation was reported for the detection of brain metastasis (43). Of note, the detection of small punctate enhancing lesions (significantly improved by the use of 3D TSE) may have an impact on patient management for a wide range of pathologies. As an example, punctiform enhancing lesions may be the first imaging sign of progressive multifocal leukoencephalopathy (PML) (44).

In case of a brain tumor adjacent to proximal arteries or dural sinuses, the black blood effect may also improve the delineation of the lesion (and thus its vascular involvement) while GRE-based techniques may be confusing. This is commonly observed in patients with meningiomas (Figure 8). Additionally, automated segmentation of the brain tumors can be easily routinely achieved using 3D TSE since adjacent vessels are systematically removed.

Meningeal enhancement

The inherent black blood effect may also improve the specificity of the 3D TSE sequence for the detection of meningeal enhancing lesions by removing the signal coming from pial/subarachnoid vessels (that may potentially lead to false-positive, especially in GRE sequences). This may be particularly useful in a wide range of pathologies including meningitis or neurosarcoidosis (Figure 7).

However, the added value of post-contrast 3D FLAIR in case of meningeal involvement is well-known. Further studies are thus required to assess the respective role of post-contrast T1W and FLAIR 3D TSE sequences for the detection of meningeal and cranial nerve enhancement.

Skull base and extracranial lesions

Because of reduced susceptibility artifacts and better image contrast, the 3D TSE sequence improves the visualization of anatomical structures located within the skull base and/or the extra-cranial soft tissues compared to GRE imaging. For instance, the intracranial and extra-cranial segments of the cranial nerves can be easily assessed using post-contrast 3D T1-w TSE (Figure 9). The use of oblique reformatted views is also useful to explore the optic nerve from the optic chiasm to the orbit (figure 10).

Of note, free-induction-decay (FID) artifacts can be encountered on TSE images, appearing as an intensity ripple in the subcutaneous fat. Such artifacts may impair the visualization of extra-cranial soft tissues but can be attenuated by increasing the spoiler (crusher) gradients or by increasing data averagingthe number of excitation.

Neurovascular diseases

Slow-flowing arterial blood as a marker of pathology. Using the post-contrast 3D T1-w TSE sequence, slow-flowing arterial blood may lead to lumen enhancement, particularly in the absence of associated MSDE or DANTE preparation. Such drawback may be useful in patients suspected of transient ischemic attack. Co-registration of the post-contrast 3D T1-w TSE sequence with SWI and contrast-enhanced MRA may be relevant in such context to better locate the vessel occlusion /stenosis (figure 11). However, since non-contrast techniques are already available to detect slow-flowing arterial blood (including 2D FLAIR or arterial spin labeling), the added value of this approach in the daily practice remains to be demonstrated. Moreover, the post-contrast T1-w sequences are not recommended at the acute stage of stroke due to the additional acquisition time.

Vessel-wall MR imaging (VW-MRI). Post-contrast high-spatial-resolution 3D T1-w TSE has emerged as the leading non-invasive imaging modality allowing for directly visualizing diseased vessel-wall. Such technique appears useful for the imaging of intracranial aneurysms and vasculitis. Indeed, VW-MRI is being increasingly used in patients with intracranial aneurysms (IA) and dedicated recommendations have recently been published (45, 46). Aneurysmal wall enhancement (AWE) is considered suggestive of instability (47-49) or rupture (47, 49-54) and may thus influence the clinical management. However, it has been recently demonstrated that residual blood flow within the aneurysmal lumen may mimic AWE on post-contrast 3D T1-w TSE images, particularly those acquired without additional blood-suppression technique (17). The use of MSDE or DANTE preparation could potentially help avoiding such pitfall (Figure 12).

Post-contrast 3D T1-w may also be of use in patients with CNS vasculitis to better detect arterial wall thickening (55). The inflammatory process is often located on small intracranial

arteries and may lead to arterial stenosis or occlusion. Compared to GRE imaging, 3D TSE allows for a better distinction between arterial wall and lumen due to the black blood effect (Figure 13).

Using post-contrast 3D T1-w TSE imaging, brain vasculitis can be distinguished from intra-cranial atheroma, which typically appears as an eccentrically arterial wall thickening and enhancement. The enhancing layer is usually considered as the fibrous cap of the atherosclerotic plaque (45).

Clinical applications of post-contrast T1w 3D TSE and GRE MR sequences are summarized in table 2.

LIMITATIONS OF THE POST-CONTRAST 3D T1-W TSE SEQUENCE

Some limitations of the 3D T1-w TSE sequence may be encountered in the clinical practice.

First, compared to GRE imaging, the low contrast between white and grey matter on 3D TSE images does not allow for a precise analysis of cortical shape/morphology (Figure 3). Indeed, ultrafast GRE MR sequences including a magnetization preparation (3D-T1-TFE, Philips Healthcare, Best, the Netherlands; BRAVO, GE Healthcare, Milwaukee, Wisconsin; MP-RAGE, Siemens, Erlangen, Germany) appear much more suitable for the detection of cortical abnormalities or to achieve brain morphometry.

Second, for the pre-operative planning of brain tumours, MRI usually includes a non-EPI fast GRE sequence (T1-FFE, Philips Healthcare, Best, the Netherlands; SPGR, GE Healthcare,

Milwaukee, Wisconsin; FLASH, Siemens, Erlangen, Germany), instead of 3D TSE, because the visualization of both brain lesion and adjacent vessels is then required.

In patients suspected of venous thrombosis, the 3D T1-w TSE sequence is usually not recommended since the black blood effect can lead to misdiagnosis a filling defect within brain veins and sinuses (Figure 14).

Finally, spontaneous T1w hyperintense lesions may mimic enhancement, for example in patients with MS. As previously suggested, for the proper evaluation of enhancement on all post-contrast images, non-enhanced images should be examined concurrently to determine whether hyperintensity is related to enhancement or intrinsic T1 shortening (56).

CONCLUSION

The post-contrast 3D T1-w TSE MR sequence may improve the sensitivity for the diagnosis of enhancing brain lesions, mainly due to an improved contrast and its inherent black blood effect. Co-registration with other 3D sequences may further improve the diagnostic work-up. The use of 3D TSE or GRE post-contrast imaging should be determined based on clinical context, each approach being associated with specific limitations.

CONFLICT OF INTEREST

The authors report no conflict of interest.

REFERENCES

1. Busse RF, Brau AC, Vu A, et al. Effects of refocusing flip angle modulation and view ordering in 3D fast spin echo. Magnetic resonance in medicine. 2008;60(3):640-9.

2. Busse RF, Hariharan H, Vu A, Brittain JH. Fast spin echo sequences with very long echo trains: design of variable refocusing flip angle schedules and generation of clinical T2 contrast. Magnetic resonance in medicine. 2006;55(5):1030-7.

3. Moraal B, Roosendaal SD, Pouwels PJ, et al. Multi-contrast, isotropic, single-slab 3D MR imaging in multiple sclerosis. European radiology. 2008;18(10):2311-20.

4. Chappell PM, Pelc NJ, Foo TK, Glover GH, Haros SP, Enzmann DR. Comparison of lesion enhancement on spin-echo and gradient-echo images. AJNR American journal of neuroradiology. 1994;15(1):37-44.

5. Mugler JP, 3rd, Brookeman JR. Three-dimensional magnetization-prepared rapid gradient-echo imaging (3D MP RAGE). Magnetic resonance in medicine. 1990;15(1):152-7.

6. Mugler JP, 3rd, Brookeman JR. Rapid three-dimensional T1-weighted MR imaging with the MP-RAGE sequence. Journal of magnetic resonance imaging : JMRI. 1991;1(5):561-7.

7. Park J, Mugler JP, 3rd, Horger W, Kiefer B. Optimized T1-weighted contrast for single-slab 3D turbo spin-echo imaging with long echo trains: application to whole-brain imaging. Magnetic resonance in medicine. 2007;58(5):982-92.

8. Mugler JP, 3rd, Bao S, Mulkern RV, et al. Optimized single-slab three-dimensional spin-echo MR imaging of the brain. Radiology. 2000;216(3):891-9.

9. Mugler JP, 3rd. Optimized three-dimensional fast-spin-echo MRI. Journal of magnetic resonance imaging : JMRI. 2014;39(4):745-67.

10. Sarkar SN, Alsop DC, Madhuranthakam AJ, et al. Brain MR imaging at ultra-low radiofrequency power. Radiology. 2011;259(2):550-7.

11. Alexander AL, Buswell HR, Sun Y, Chapman BE, Tsuruda JS, Parker DL. Intracranial black-blood MR angiography with high-resolution 3D fast spin echo. Magnetic resonance in medicine. 1998;40(2):298-310.

12. Jara H, Yu BC, Caruthers SD, Melhem ER, Yucel EK. Voxel sensitivity function description of flow-induced signal loss in MR imaging: implications for black-blood MR angiography with turbo spin-echo sequences. Magnetic resonance in medicine. 1999;41(3):575-90.

13. Qiao Y, Steinman DA, Qin Q, et al. Intracranial arterial wall imaging using three-dimensional high isotropic resolution black blood MRI at 3.0 Tesla. Journal of magnetic resonance imaging : JMRI. 2011;34(1):22-30.

14. Kallmes DF, Hui FK, Mugler JP, 3rd. Suppression of cerebrospinal fluid and blood flow artifacts in FLAIR MR imaging with a single-slab three-dimensional pulse sequence: initial experience. Radiology. 2001;221(1):251-5.

15. Xie Y, Yang Q, Xie G, Pang J, Fan Z, Li D. Improved black-blood imaging using DANTE-SPACE for simultaneous carotid and intracranial vessel wall evaluation. Magnetic resonance in medicine. 2016;75(6):2286-94.

16. Zhu C, Graves MJ, Yuan J, Sadat U, Gillard JH, Patterson AJ. Optimization of improved motion-sensitized driven-equilibrium (iMSDE) blood suppression for carotid artery wall imaging. Journal of cardiovascular magnetic resonance : official journal of the Society for Cardiovascular Magnetic Resonance. 2014;16:61.

17. Kalsoum E, Chabernaud Negrier A, Tuilier T, et al. Blood Flow Mimicking Aneurysmal Wall Enhancement: A Diagnostic Pitfall of Vessel Wall MRI Using the

Postcontrast 3D Turbo Spin-Echo MR Imaging Sequence. AJNR American journal of neuroradiology. 2018;39(6):1065-7.

18. Fan Z, Zhang Z, Chung YC, et al. Carotid arterial wall MRI at 3T using 3D variable-flip-angle turbo spin-echo (TSE) with flow-sensitive dephasing (FSD). Journal of magnetic resonance imaging : JMRI. 2010;31(3):645-54.

19. Wang J, Yarnykh VL, Hatsukami T, Chu B, Balu N, Yuan C. Improved suppression of plaque-mimicking artifacts in black-blood carotid atherosclerosis imaging using a multislice motion-sensitized driven-equilibrium (MSDE) turbo spin-echo (TSE) sequence. Magnetic resonance in medicine. 2007;58(5):973-81.

20. Su S, Ren Y, Shi C, et al. Black-blood T2* mapping with delay alternating with nutation for tailored excitation. Magnetic resonance imaging. 2017;40:91-7.

21. Li L, Chai JT, Biasiolli L, et al. Black-blood multicontrast imaging of carotid arteries with DANTE-prepared 2D and 3D MR imaging. Radiology. 2014;273(2):560-9.

22. Li L, Miller KL, Jezzard P. DANTE-prepared pulse trains: a novel approach to motion-sensitized and motion-suppressed quantitative magnetic resonance imaging. Magnetic resonance in medicine. 2012;68(5):1423-38.

23. Pruessmann KP, Weiger M, Scheidegger MB, Boesiger P. SENSE: sensitivity encoding for fast MRI. Magnetic resonance in medicine. 1999;42(5):952-62.

24. Breuer FA, Blaimer M, Mueller MF, et al. Controlled aliasing in volumetric parallel imaging (2D CAIPIRINHA). Magnetic resonance in medicine. 2006;55(3):549-56.

25. Fritz J, Fritz B, Thawait GG, Meyer H, Gilson WD, Raithel E. Three-Dimensional CAIPIRINHA SPACE TSE for 5-Minute High-Resolution MRI of the Knee. Investigative radiology. 2016;51(10):609-17.

26. Geethanath S, Reddy R, Konar AS, et al. Compressed sensing MRI: a review. Critical reviews in biomedical engineering. 2013;41(3):183-204.

27. Vasanawala SS, Alley MT, Hargreaves BA, Barth RA, Pauly JM, Lustig M. Improved pediatric MR imaging with compressed sensing. Radiology. 2010;256(2):607-16.

28. Toledano-Massiah S, Sayadi A, de Boer R, et al. Accuracy of the Compressed Sensing Accelerated 3D-FLAIR Sequence for the Detection of MS Plaques at 3T. AJNR American journal of neuroradiology. 2018;39(3):454-8.

29. Kayvanrad M, Lin A, Joshi R, Chiu J, Peters T. Diagnostic quality assessment of compressed sensing accelerated magnetic resonance neuroimaging. Journal of magnetic resonance imaging : JMRI. 2016;44(2):433-44.

30. Dolezal O, Dwyer MG, Horakova D, et al. Detection of cortical lesions is dependent on choice of slice thickness in patients with multiple sclerosis. International review of neurobiology. 2007;79:475-89.

31. Molyneux PD, Tubridy N, Parker GJ, et al. The effect of section thickness on MR lesion detection and quantification in multiple sclerosis. AJNR American journal of neuroradiology. 1998;19(9):1715-20.

32. Bink A, Schmitt M, Gaa J, Mugler JP, 3rd, Lanfermann H, Zanella FE. Detection of lesions in multiple sclerosis by 2D FLAIR and single-slab 3D FLAIR sequences at 3.0 T: initial results. European radiology. 2006;16(5):1104-10.

33. Yoon BC, Saad AF, Rezaii P, Wintermark M, Zaharchuk G, Iv M. Evaluation of Thick-Slab Overlapping MIP Images of Contrast-Enhanced 3D T1-Weighted CUBE for Detection of Intracranial Metastases: A Pilot Study for Comparison of Lesion Detection, Interpretation Time, and Sensitivity with Nonoverlapping CUBE MIP, CUBE, and Inversion-Recovery-Prepared Fast-Spoiled Gradient Recalled Brain Volume. AJNR American journal of neuroradiology. 2018;39(9):1635-42.

34. Reichert M, Morelli JN, Runge VM, et al. Contrast-enhanced 3-dimensional SPACE versus MP-RAGE for the detection of brain metastases: considerations with a 32-channel head coil. Investigative radiology. 2013;48(1):55-60.

35. Hodel J, Outteryck O, Ryo E, et al. Accuracy of postcontrast 3D turbo spin-echo MR sequence for the detection of enhanced inflammatory lesions in patients with multiple sclerosis. AJNR American journal of neuroradiology. 2014;35(3):519-23.

36. Lee S, Park DW, Lee JY, Lee YJ, Kim T. Improved motion-sensitized driven-equilibrium preparation for 3D turbo spin echo T1 weighted imaging after gadolinium administration for the detection of brain metastases on 3T MRI. The British journal of radiology. 2016;89(1063):20150176.

37. Melki PS, Jolesz FA, Mulkern RV. Partial RF echo-planar imaging with the FAISE method. II. Contrast equivalence with spin-echo sequences. Magnetic resonance in medicine. 1992;26(2):342-54.

38. Melki PS, Jolesz FA, Mulkern RV. Partial RF echo planar imaging with the FAISE method. I. Experimental and theoretical assessment of artifact. Magnetic resonance in medicine. 1992;26(2):328-41.

39. Aboukais R, Zairi F, Bourgeois P, et al. Clinical and imaging follow-up after surgical or endovascular treatment in patients with unruptured carotid-ophthalmic aneurysm. Clinical neurology and neurosurgery. 2014;125:155-9.

40. Kato Y, Higano S, Tamura H, et al. Usefulness of contrast-enhanced T1-weighted sampling perfection with application-optimized contrasts by using different flip angle evolutions in detection of small brain metastasis at 3T MR imaging: comparison with magnetization-prepared rapid acquisition of gradient echo imaging. AJNR American journal of neuroradiology. 2009;30(5):923-9.

41. Kumar S, Kumar S, Surya M, Mahajan A, Sharma S. To Compare Diagnostic Ability of Contrast-Enhanced Three-Dimensional T1-SPACE with Three-Dimensional Fluid-Attenuated Inversion Recovery and Three-Dimensional T1-Magnetization Prepared Rapid Gradient Echo Magnetic Resonance Sequences in Patients of Meningitis. Journal of neurosciences in rural practice. 2019;10(1):48-53.

42. Jeevanandham B, Kalyanpur T, Gupta P, Cherian M. Comparison of post-contrast 3D-T1-MPRAGE, 3D-T1-SPACE and 3D-T2-FLAIR MR images in evaluation of meningeal abnormalities at 3-T MRI. The British journal of radiology. 2017;90(1074):20160834.

43. Kim D, Heo YJ, Jeong HW, et al. Usefulness of the Delay Alternating with Nutation for Tailored Excitation Pulse with T1-Weighted Sampling Perfection with Application-Optimized Contrasts Using Different Flip Angle Evolution in the Detection of Cerebral Metastases: Comparison with MPRAGE Imaging. AJNR American journal of neuroradiology. 2019.

44. Hodel J, Darchis C, Outteryck O, et al. Punctate pattern: A promising imaging marker for the diagnosis of natalizumab-associated PML. Neurology. 2016;86(16):1516-23.

45. Mandell DM, Mossa-Basha M, Qiao Y, et al. Intracranial Vessel Wall MRI: Principles and Expert Consensus Recommendations of the American Society of Neuroradiology. AJNR American journal of neuroradiology. 2017;38(2):218-29.

46. Lehman VT, Brinjikji W, Mossa-Basha M, et al. Conventional and high-resolution vessel wall MRI of intracranial aneurysms: current concepts and new horizons. Journal of neurosurgery. 2017:1-13.

47. Edjlali M, Gentric JC, Regent-Rodriguez C, et al. Does aneurysmal wall enhancement on vessel wall MRI help to distinguish stable from unstable intracranial aneurysms? Stroke. 2014;45(12):3704-6.

48. Fu Q, Guan S, Liu C, Wang K, Cheng J. Clinical Significance of Circumferential Aneurysmal Wall Enhancement in Symptomatic Patients with Unruptured Intracranial Aneurysms: a High-resolution MRI Study. Clinical neuroradiology. 2017.

49. Hu P, Yang Q, Wang DD, Guan SC, Zhang HQ. Wall enhancement on high-resolution magnetic resonance imaging may predict an unsteady state of an intracranial saccular aneurysm. Neuroradiology. 2016;58(10):979-85.

50. Endo H, Niizuma K, Fujimura M, et al. Ruptured Cerebral Microaneurysm Diagnosed by 3-Dimensional Fast Spin-Echo T1 Imaging with Variable Flip Angles. Journal of stroke and cerebrovascular diseases : the official journal of National Stroke Association. 2015;24(8):e231-5.

51. Nagahata S, Nagahata M, Obara M, et al. Wall Enhancement of the Intracranial Aneurysms Revealed by Magnetic Resonance Vessel Wall Imaging Using Three-Dimensional Turbo Spin-Echo Sequence with Motion-Sensitized Driven-Equilibrium: A Sign of Ruptured Aneurysm? Clinical neuroradiology. 2016;26(3):277-83.

52. Omodaka S, Endo H, Niizuma K, et al. Quantitative Assessment of Circumferential Enhancement along the Wall of Cerebral Aneurysms Using MR Imaging. AJNR American journal of neuroradiology. 2016;37(7):1262-6.

53. Omodaka S, Endo H, Niizuma K, et al. Circumferential Wall Enhancement on Magnetic Resonance Imaging is Useful to Identify Rupture Site in Patients with Multiple Cerebral Aneurysms. Neurosurgery. 2017.

54. Matouk CC, Mandell DM, Gunel M, et al. Vessel wall magnetic resonance imaging identifies the site of rupture in patients with multiple intracranial aneurysms: proof of principle. Neurosurgery. 2013;72(3):492-6; discussion 6.

55. Zeiler SR, Qiao Y, Pardo CA, Lim M, Wasserman BA. Vessel Wall MRI for Targeting Biopsies of Intracranial Vasculitis. AJNR American journal of neuroradiology. 2018;39(11):2034-6.

56. Janardhan V, Suri S, Bakshi R. Multiple sclerosis: hyperintense lesions in the brain on nonenhanced T1-weighted MR images evidenced as areas of T1 shortening. Radiology. 2007;244(3):823-31.

CE-3D-T1	**TSE** (CUBE/SPACE/ VISTA/ BRAINVIEW)	**Non-EPI fast GRE** (SPGR/FLASH/FFE)	**Ultrafast GRE with magnetization-preparation** (BRAVO/MP-RAGE/TFE)
Contrast between grey and white matter	Very low	Low	High
Flow sensitivity	Low	High	High
Artifacts from static field inhomogeneity	Reduced	Present	Present
Fat suppression	Usually performed	Usually not performed	Usually not performed

Table 1. Technical differences between TSE and GRE MR sequences

CE-3D-T1	**TSE** (CUBE/SPACE/ VISTA/ BRAINVIEW)	**Non-EPI fast GRE** (SPGR/FLASH/FFE)	**Ultrafast GRE with magnetization-preparation** (BRAVO/MP-RAGE/TFE)
Contrast/detection of brain enhancing lesions	+++	++	+
Detection of brain meningeal/nerve lesions	+++	+	+
Sensitivity to slow-flowing blood	+++	0	0
Vessel-wall analysis	+++	0	0
Visualization of brain vessel lumen (arteries and veins)	0	+++	+++
Morphological analysis – distinction between GM and WM	+	++	+++

Table 2 : Clinical applications of post-contrast T1w 3D TSE and GRE MR sequences

FIGURE CAPTIONS

Figure 1: Minimal Intensity Projection (MinIP) axial (A) and coronal (B) reformatted views from 3D T1-w TSE images. Note the homogeneous and complete hypointensity of brain arteries (the "black blood" effect).

Figure 2: Comparison between axial 2D (A) and 3D (B) post-contrast TSE images in a 34 year-old patient with MS. Two millimetric enhanced MS lesions are visible in the cerebellum (B, arrowheads) on post-contrast 3D T1-w TSE image. These lesions were previously hindered by flow-related artifacts on 2D TSE images (A, arrows).

Figure 3: Comparison between contrast-enhanced MR angiography (A), 3D T1w magnetization-prepared GRE (B), non-EPI fast GRE sequence (C) and 3D T1 TSE (D) of a normal brain. Note the black blood effect within the superior sagittal sinus (D, arrowhead) and brain arteries (D, arrow) on 3D TSE image, while the vessels appear enhanced with all other sequences (A, B and C, arrows and arrowheads). The contrast between white and gray matter is a very low on 3D T1 TSE images (D), low on non-EPI fast GRE (C) and high on 3D T1 magnetization-prepared GRE images (B).

Figure 4: Comparison between post-contrast 3D T1-w TSE without (A) and with Motion-Sensitized Driven-Equilibrium (MSDE) (B). The lumen of the venous sinuses appears enhanced using 3D T1-w TSE sequence performed without MSDE (A, arrows). Note

the drastic reduction of enhancement in the transverse sinuses when adding the MDSE preparation (B, arrowheads).

Figure 5: Axial 4-mm slice thickness (A), 1-mm source image (B) and MIP reformation (C) from post-contrast 3D T1-w TSE sequence in a 43 year-old patient with MS. A left periventricular small MS lesion detected on source and MIP images (B and C, arrows) was missed on 4mm thick section image (A, arrowhead) due to the partial volume effect.

Figure 6: Co-registration of post-contrast 3D T1-w TSE (MIP 5mm) (A) with pre-contrast 3D DIR (B) and axial SWI (MinIP 5mm) (C) in a 33 year-old patient with MS. The enhancing MS lesion (A, arrowhead) corresponds to a hyperintensity on T2-w DIR images (B, arrowhead). The developmental venous anomaly (A, arrow) also appears enhanced on 3D TSE images (A, arrow) is nicely demonstrated on SWI (C, arrow) without any hyperintensity visible on T2-w DIR images.

Figure 7: Comparison between post-contrast 3D T1-w GRE (A) versus 3D T1-w TSE (B) in a 62 year-old patient with neurosarcoïdis. Using GRE imaging, both pial vessels and granulomas (A, arrowheads) appear enhanced. Leptomeningeal enhancement is more precisely delineated using the 3D T1-w TSE sequence (B, arrowheads) due to the removal of pial vessel signal. Note the arterial and venous black blood effect and low white/gray-matter contrast on 3D T1-w TSE image (B).

Figure 8: Post-contrast 3D T1-w GRE (A) and TSE (B) sequences after surgical resection of a pineal-region meningioma in a 60-year-old patient. Using GRE imaging, the tumoral remnant (A, arrow), close to great cerebral vein (A, arrowheads), was misdiagnosed. Using TSE imaging, the black blood effect improves the distinction between the remnant (B, arrow) and the adjacent vein (B, arrowheads).

Post-contrast 3D T1-w GRE (C) and TSE (D) sequences in a 51-year-old patient with meningioma adjacent to the left lateral sinus. Using GRE imaging, the distinction between between the meningioma (C, arrow) and the adjacent lateral sinus (C, arrowhead) is difficult. Using TSE imaging, thanks to the black blood effect, the meningioma (D, arrow) is easily distinguished from the adjacent vein (D, arrowhead).

Figure 9: 22-year-old man with left facial palsy. The extra-cranial segments of the cranial nerves can be easily assessed thanks to the multiplanar reformats (MPR) and MIP reconstructions. Using 3D TSE images, a contrast enhancement of the first (A, arrow) and second (A, arrowhead) portions of the left VII nerve is visible. The abnormal enhanced extra cranial segment of the nerve is well studied on both MPR (B) and MIP (C) reconstructions (arrows).

Figure 10: 43-year-old patient with left optic neuritis. Multiplanar reformats from post-contrast 3D T1-w TSE images demonstrate contrast enhancement of the subarachnoid segment of the left optic nerve (A and B, arrow).

Figure 11: 54-year-old man admitted for a suspected tansient ischemic attack (TIA). FLAIR image (A) shows a subtle hyperintense vascular hyperintensity (arrows) while post-contrast 3D T1 TSE image (B) revealed extensive vascular enhancement related to slow-flowing arterial blood (arrows). Contrast-enhanced MRA confirmed the occlusion of the left middle cerebral artery (C, arrow). In such case, the 3D T1-w TSE sequence, by enhancing slow-flowing arterial blood, may improve the detection of arterial occlusion on CE-MRA images.

Figure 12: 34-year-old man with a large intracranial aneurysm of the ophthalmic segment of the right internal carotid artery. Time-of-flight (TOF) MR image (A) and conventional angiograms (D, E, F) show turbulent flow in the lumen of the aneurysm (arrows). Post-contrast 3D T1-w TSE image without additional blood-suppression techniques (B) show enhanced both turbulent flows and thick pseudo-enhancement of the aneurysmal wall (arrows). 3D T1-w TSE image with additional black blood technique (MDSE) (C) demonstrates only a slight contrast enhancement of the aneurysmal wall (arrows) due to the improved suppression of flowing-blood.

Figure 13: 47-year-old woman with a cerebral arteritis, post-contrast 3D T1-w GRE (A) and TSE (B, C) images. Conventional angiogram (D) and time-of-flight (TOF) MR angiography (E) at the acute phase show a focal stenosis of the middle cerebral artery (arrows). The post-contrast 3D T1-w GRE sequence (A) cannot distinguish the inflammatory process of the arterial wall (wall enhancement, arrow) from the enhanced arterial lumen (arrowhead). On the opposite, the post-contrast 3D T1-w TSE sequence (B) nicely distinguishes the arterial wall enhancement at the site of the stenosis (arrow) from the normal

arterial lumen upstream appears hypointense (arrowhead) thanks to the black blood effect. After corticotherapy, signal abnormalities on both post-contrast 3D T1-w TSE (C) and TOF (F) sequences returned to normal.

Figure 14: 65-year-old patient with thrombosis of the right transverse sinus. The subtracted contrast-enhanced MR angiographic sequence at the venous phase (A) shows a focal defect of contrast filling in the right transverse sinus (arrowhead) related to the venous thrombosis. Due to its inherent black blood effect, the post-contrast 3D T1-w TSE sequence cannot separate the normal venous lumen (B, arrows) from the venous thrombus (B, arrowhead). Indeed, the use of 3D TSE is not recommended for the diagnosis of cerebral venous thrombosis.

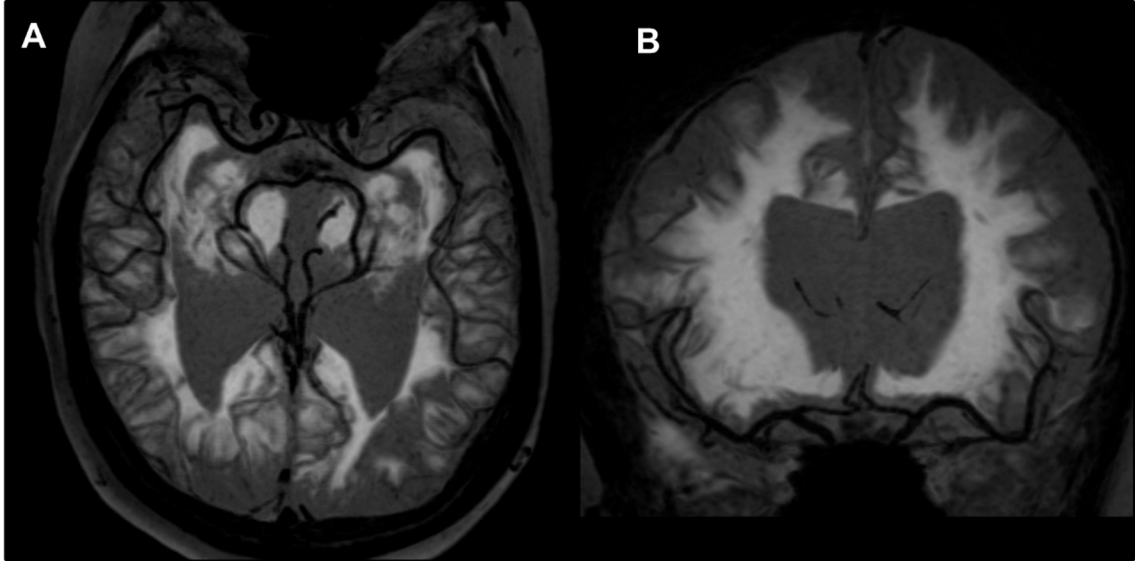
A
B

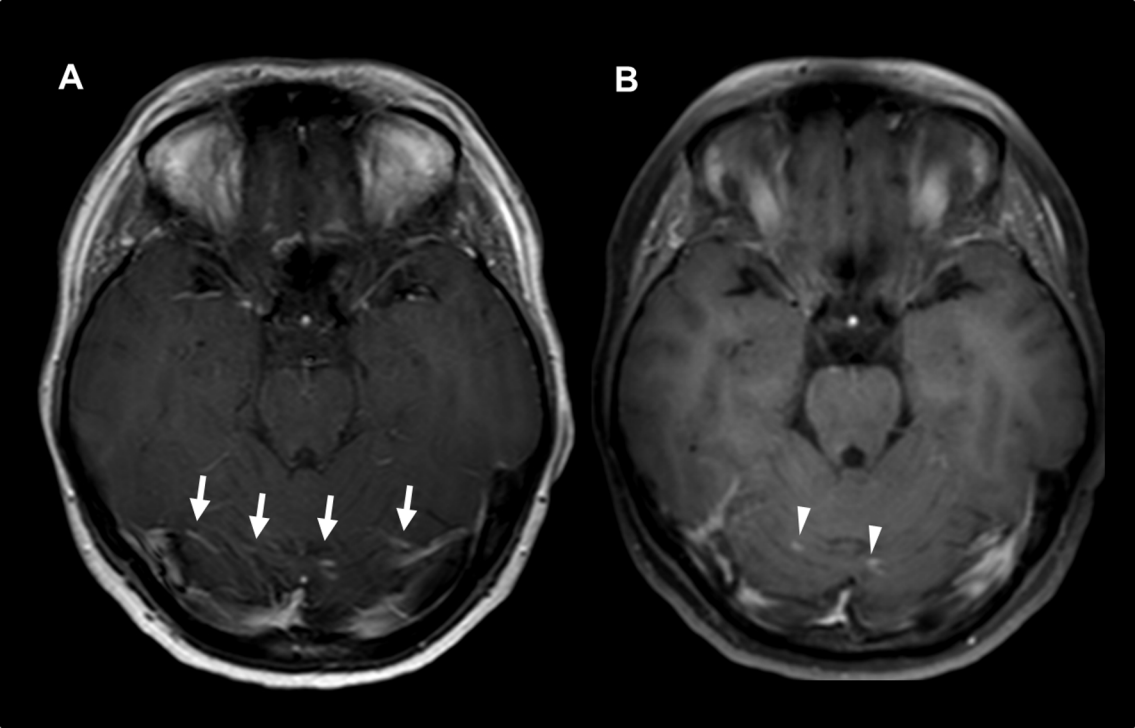
A
B

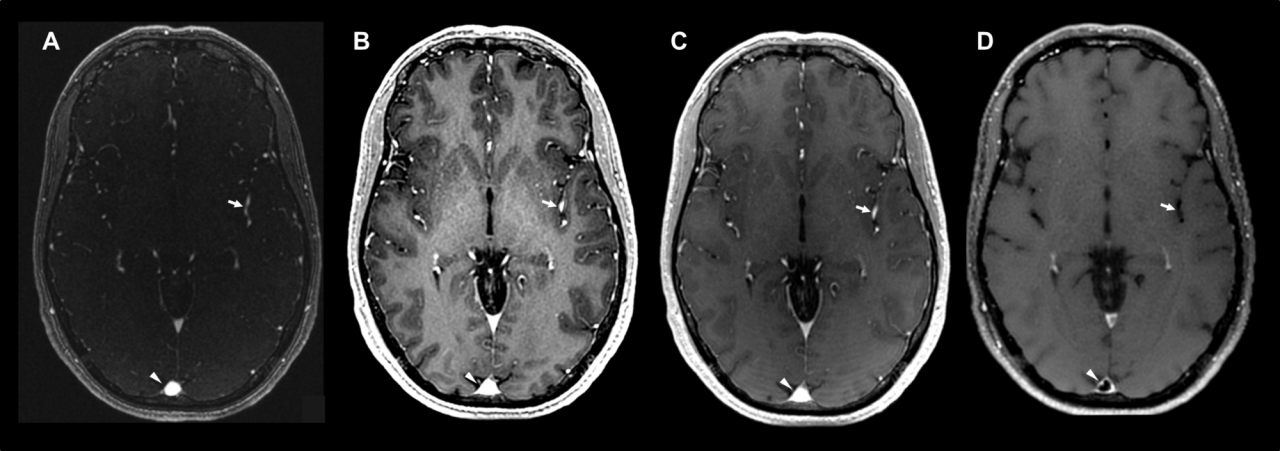
A
B
C
D

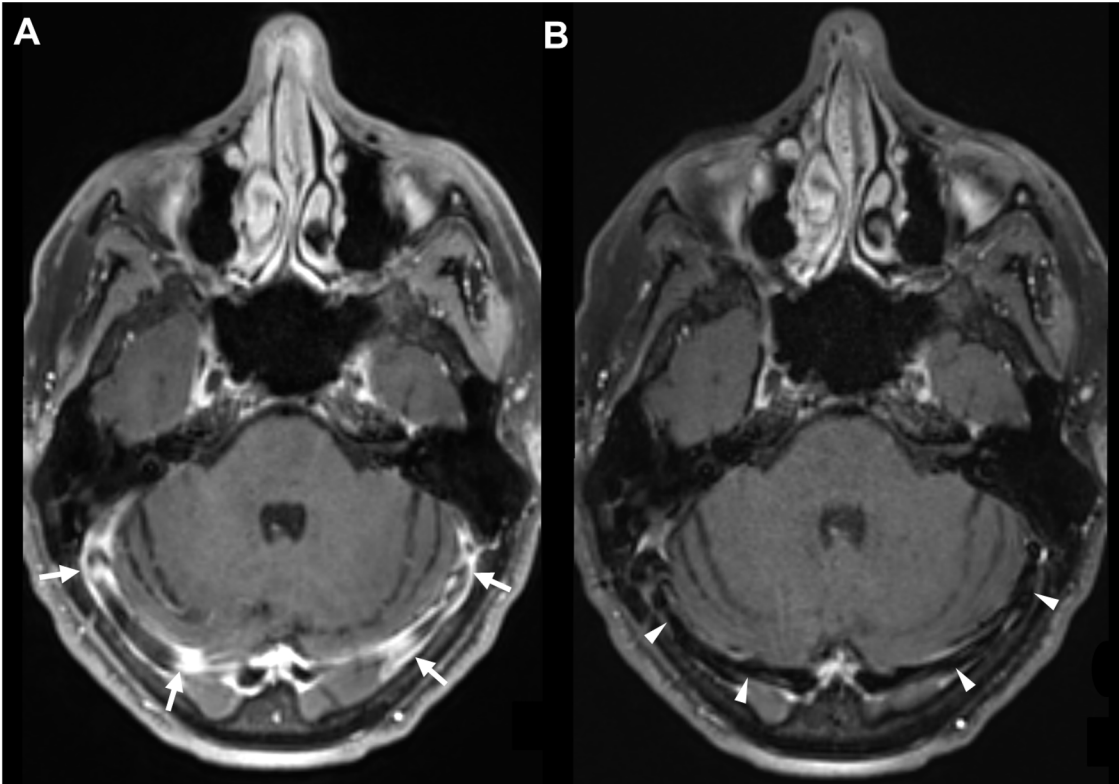
A
B

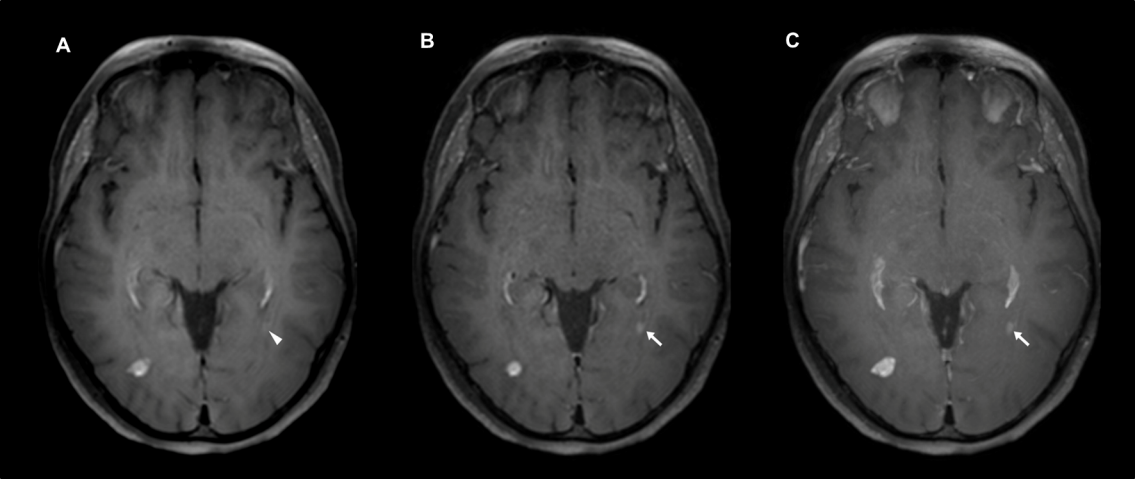
A
B
C

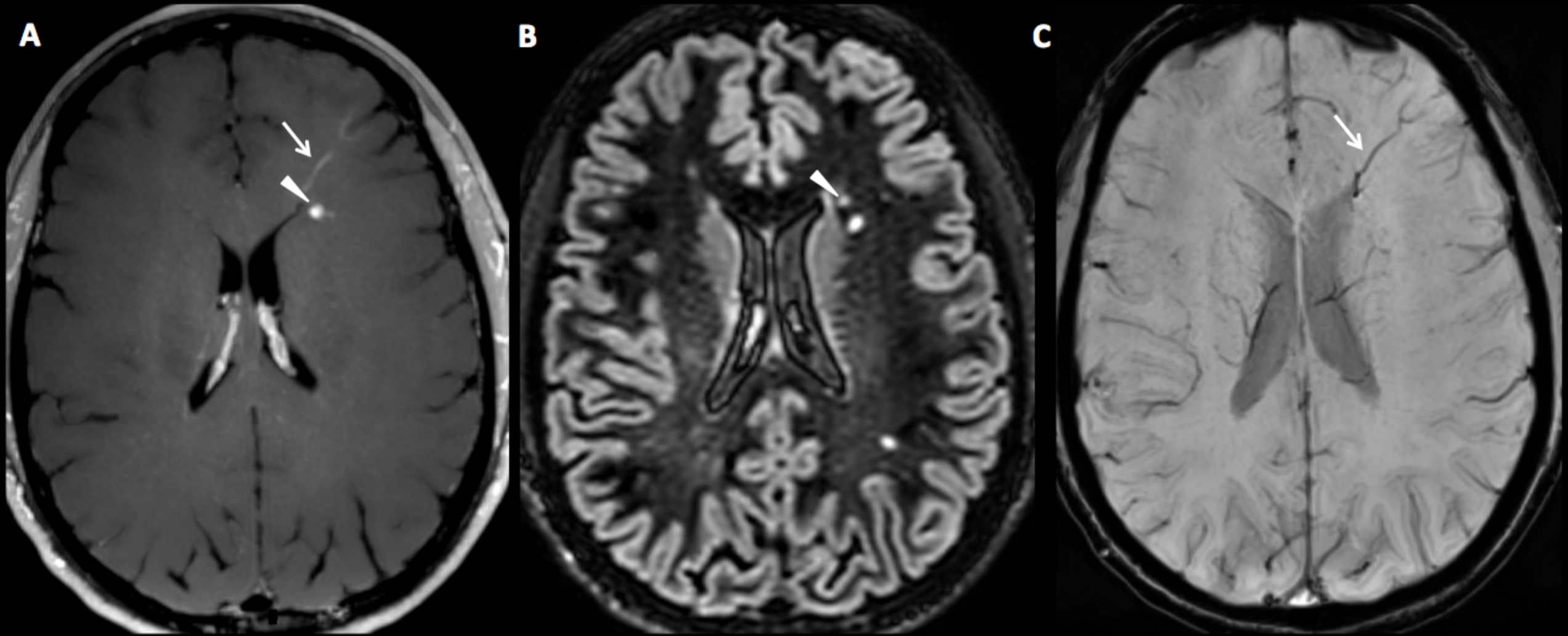
A
B
C

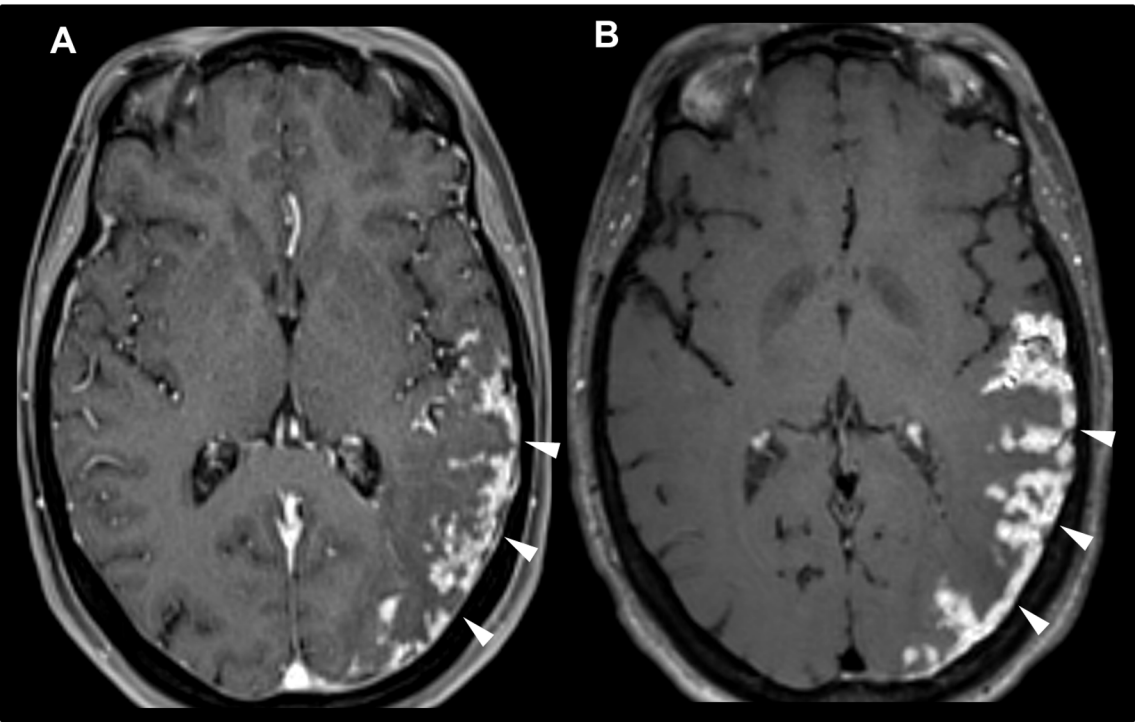
A
B

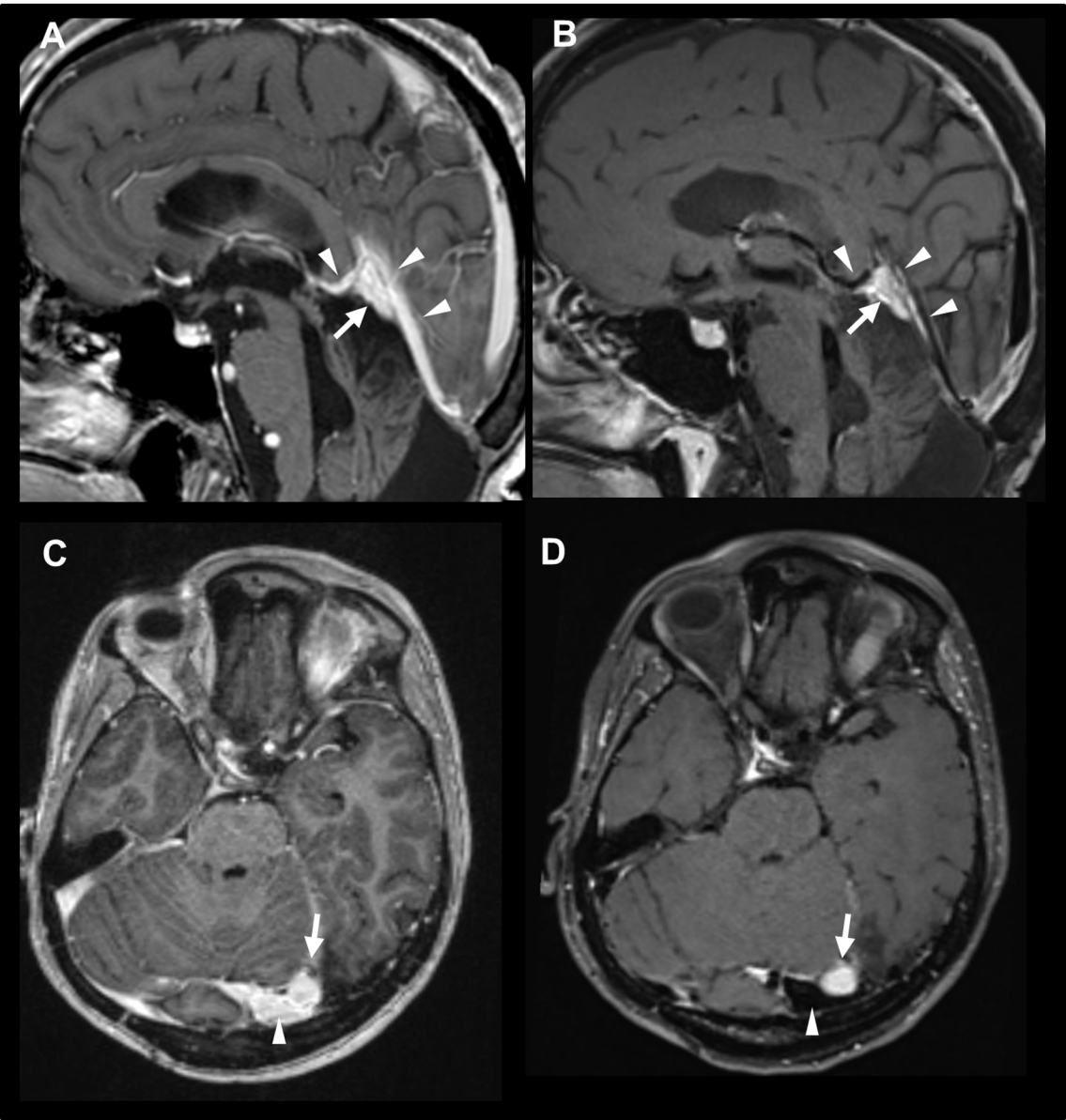
A
B
C
D

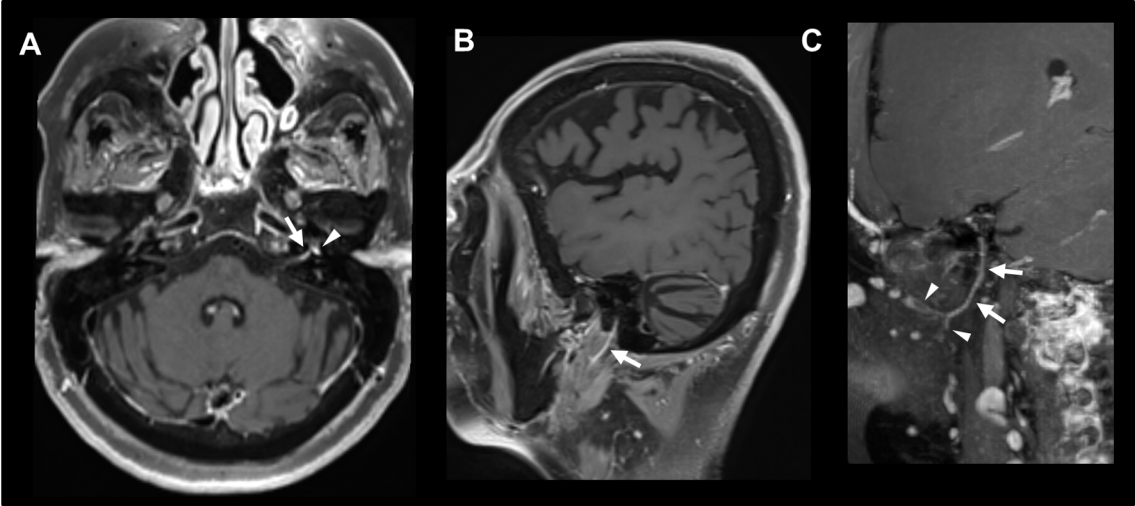
A
B
C

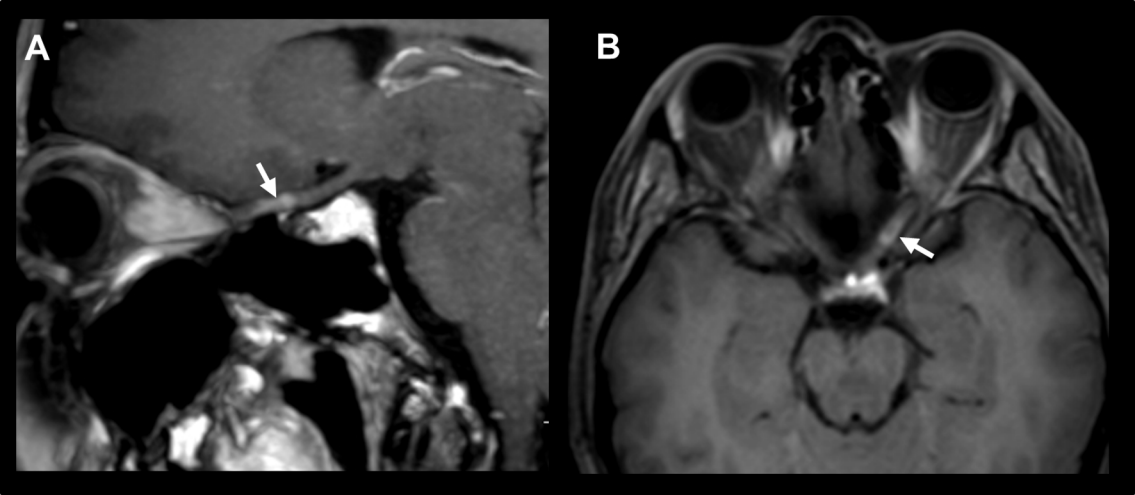
A
B

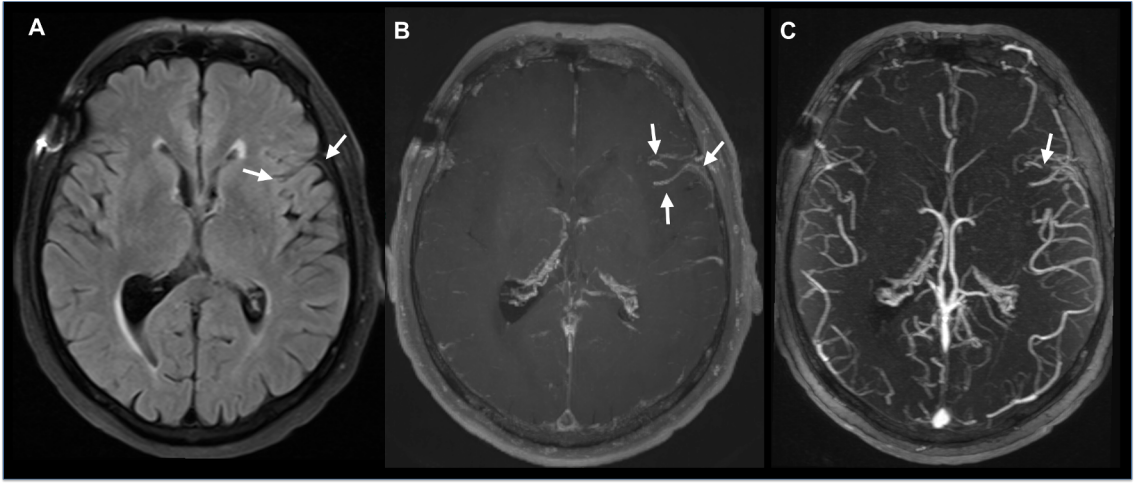
A
B
C

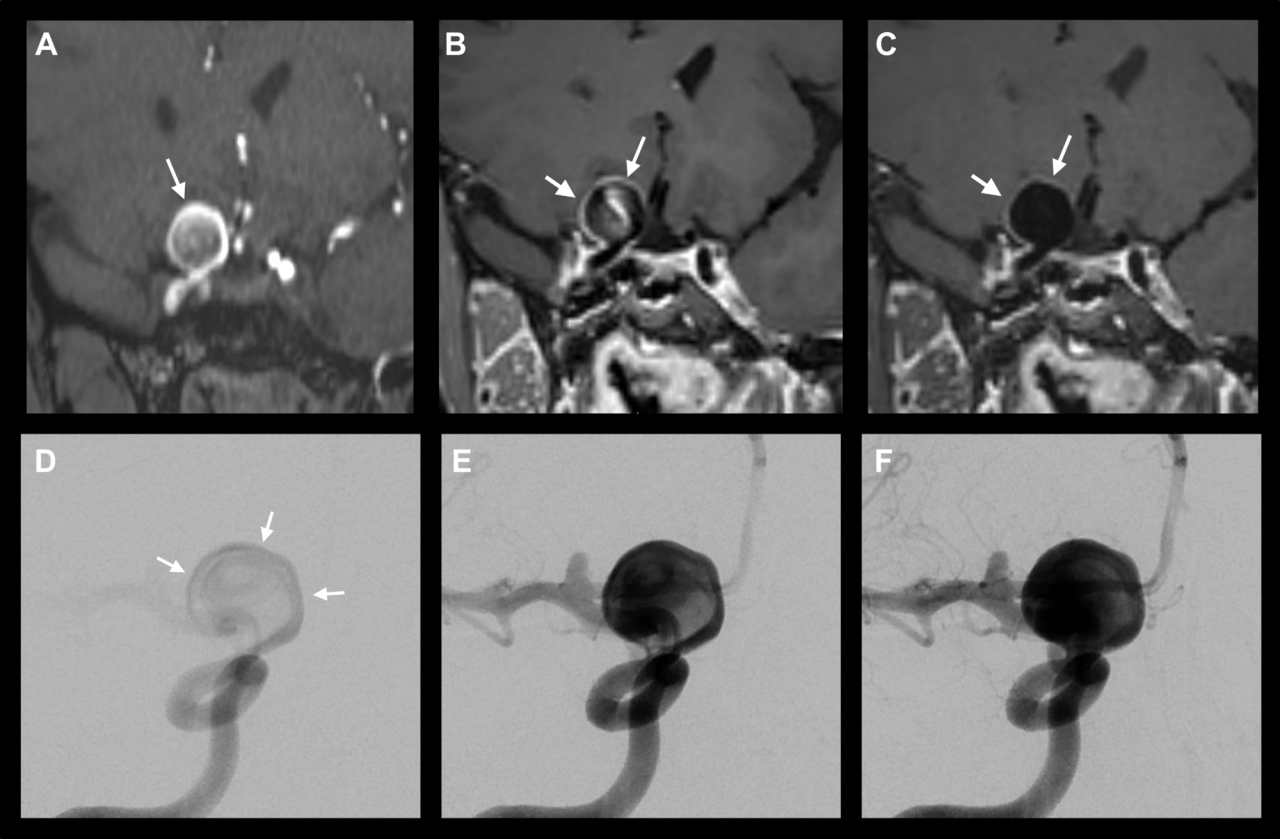
A
B
C
D
E
F

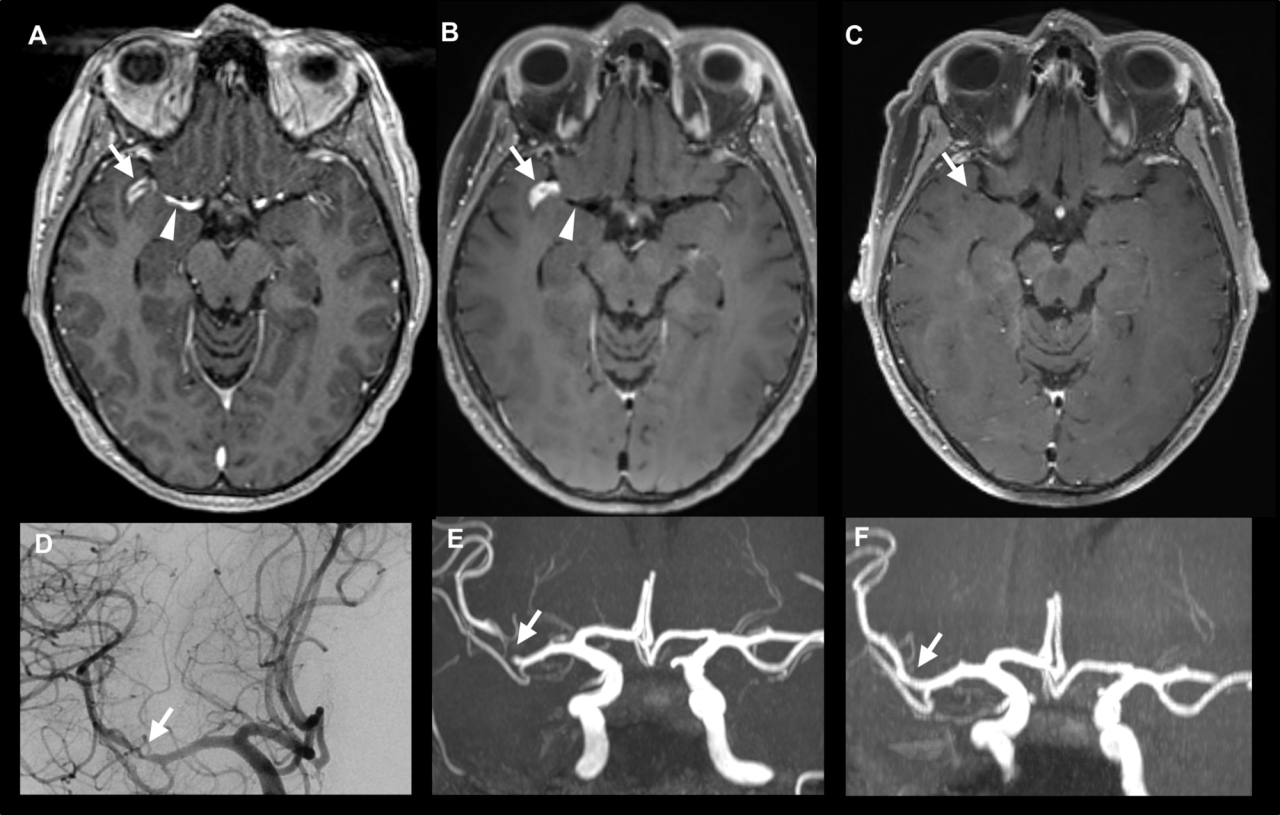
A
B
C
D
E
F

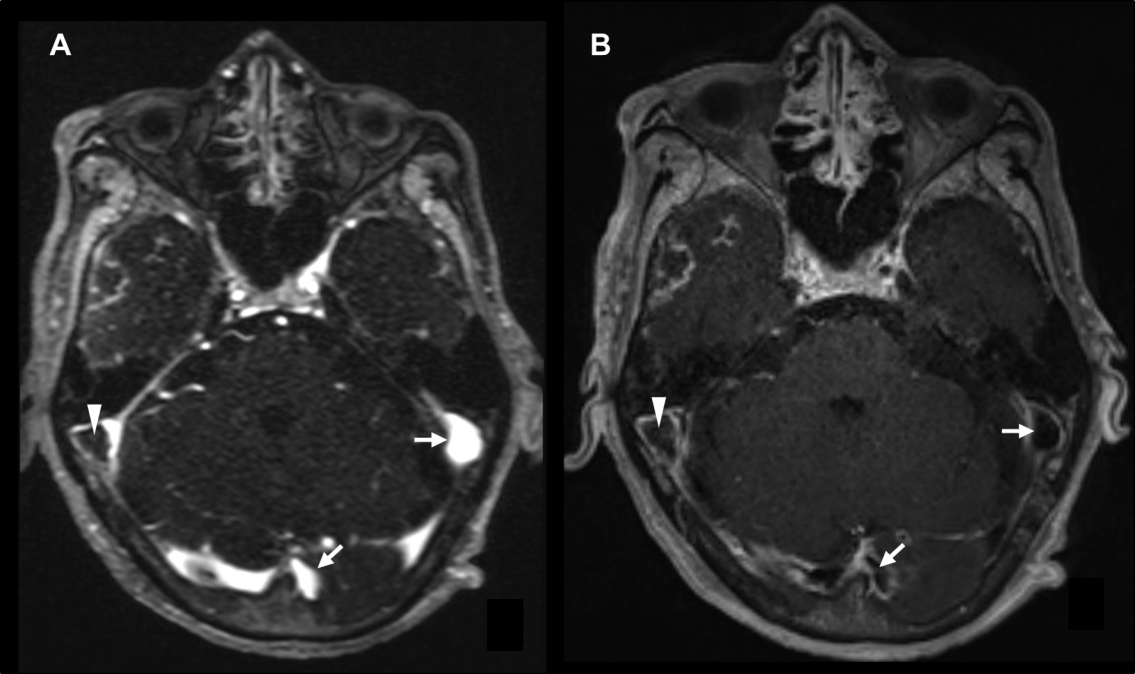
A
B